Comparative Immunology, Microbiology and Infectious Diseases 63 (2019) 44–50

Contents lists available at ScienceDirect

Comparative Immunology, Microbiology and Infectious Diseases

journal homepage: www.elsevier.com/locate/cimid

Disruption of blood-brain barrier by an *Escherichia coli* isolated from canine septicemia and meningoencephalitis

Xin Li[a,1], Zecai Zhang[a,b,1], Xiaoran Chang[a,1], Xu Wang[a], Junying Hu[a], Qian Lin[a], Yingqi Jia[a], Xu Yang[a], Xinping Wang[a,b,*]

[a] College of Veterinary Medicine, Jilin University, Changchun, Jilin, China
[b] Key laboratory for Zoonoses Research, Ministry of Education, Changchun, Jilin, China

ARTICLE INFO

Keywords:
Dogs
Escherichia coli
Septicemia
Meningoencephalitis
Blood-brain barrier

ABSTRACT

Escherichia coli (E. coli) is one of the common pathogenic bacteria in veterinary clinical infection. As an opportunistic microorganism, *E. coli* normally does not cause diseases. However, it causes infections under certain circumstance to domesticated animal and poultry, resulting in severe diarrhea, septicemia, and respiratory infections. Although there are increasing reports regarding the infections of *E. coli* to domestic animals and poultry, the infection of *E. coli* in dogs is relatively less reported, especially on septicemia and meningoencephalitis. Here, we reported the isolation and identification of an *E. coli* isolate named CEC-GZL17 from dogs characterized by septicemia and sudden death, and found that CEC-GZL17 is able to cause meningoencephalitis. Exploration on the potential mechanism underlying meningoencephalitis demonstrated that CEC-GZL17 infection significantly increases TNF-α expression and inhibits ZO-1 and occludin expressions in brain tissue, indicating that the *E coli* likely use the mechanism to penetrate the blood-brain barrier via disrupting tight junction architecture, thus leading to the invasion to brain tissue.

1. Introduction

Escherichia coli (*E. coli*) is a Gram-negative, rod-shaped and coliform bacterium that is widely existed in human and animal gut and natural environment [1]. As one of the most common and important opportunistic microorganisms, *E. coli* infects many animal species, which poses a severe threat to public health and the livestock industry. Animals infected by *E. coli* normally manifest multiple clinical signs including severe respiratory infections, diarrhea and sepsis [2–4]. In addition, *E.coli* infection also cause the meningoencephalitis in human and animals, resulting in a relatively high mortality [5,6]. Although *E. coli* infection has been reported frequently in a variety of animal species, it is less reported in dogs, especially on dogs with septicemia and meningoencephalitis [7].

Under physiological conditions, access of pathogens to the central nervous system (CNS) is restricted by blood-brain barrier. However, once entering CNS, the pathogens has the ability to cause meningoencephalitis. The structural and functional integrity of blood-brain barrier depends on the polarized microvascular endothelial cells that possess tight junction (TJ) with the astrocytes surrounding the capillary. Previous study showed that abnormal expression of TJ proteins, including down-regulation of ZO-1, is a significant factor contributing to the altered permeability of blood-brain barrier [8,9]. In addition, increasing evidence suggested that local brain immune response to meningoencephalitis is associated with release of cytokines [10,11], and high expression of pro-inflammatory cytokines increases the permeability of the blood brain barrier [12]. It has been demonstrated that nuclear factor-κB (NF-κB) is involved in numerous diseases via inducing the production of pro-inflammatory cytokines such as tumor necrosis factor-α (TNF-α) [13,14]. Several studies demonstrated that activation of NF-κB pathway is also closely related to the permeability of blood brain barrier [15,16]. Although it has been reported that bacterial meningoencephalitis is associated with the increased permeability and the dysfunction of the blood-brain barrier, the mechanism and the relevant immunological factors involved in CEC-GZL17 infection remain unclear.

In this study, we reported an *E. coli* infection in dogs characterized by septicemia, meningoencephalitis, and sudden death via epidemiological investigation, pathological examination, pathogen isolation and identification, and found the isolated *E. coli* bacteria have the capacity

* Corresponding author at: Key laboratory for Zoonoses Research, Ministry of Education, College of Veterinary Medicine, Jilin University, 5333 Xian Road, Changchun, Jilin 130062, China.
E-mail address: drxwang@jlu.edu.cn (X. Wang).
[1] These authors contributed equally to this work.

https://doi.org/10.1016/j.cimid.2019.01.002
Received 25 May 2018; Received in revised form 5 January 2019; Accepted 7 January 2019

of penetrating the blood brain barrier and causing meningoencephalitis through a mechanism of down-regulating the expression of tight junction molecules. These findings provided the necessary evidence that *E. coli* as a pathogen has the capacity of causing meningoencephalitis in dogs.

2. Materials and methods

2.1. Ethics statement

Mice and the procedures used for this study were following a standard protocol reviewed and approved by the Institutional Animal Care and Use Committee (IACUC) of Jilin University (approval no JLU-20150226), following strict compliance with requirements of the Animal Ethics Procedures and Guidelines of the People's Republic of China.

2.2. Mice

Twenty-five mice (Kunming strain) obtained from Changchun Biological Products Institute were divided randomly into five groups (I to V) with 5 mice caged in each group. Mice were maintained in the Laboratory Animal Facility of Jilin University. All mice had free access to food and water and were kept in a temperature-controlled room (22 ± 0.5 °C). The infected mice were euthanized by CO_2 inhalation and dislocation after showing clinical signs and dissected in a biosafety II Cabinet following a standard procedure.

2.3. Electron microscopy observation

Tissue samples from the necrotized dogs including lung, liver, spleen, brain, kidney and lymph nodes were processed for detection of potential viral pathogens using Electron Microscopy following the procedure as previously described [17].

2.4. Isolation and characterization

Potential bacteria were examined by observing the smear slides prepared from samples of liver, spleen, lung, brain, pericardial fluid, and blood following a standard sterilized procedure. The slides were stained with Gram staining method and examined using light microscopy.

Characterization of bacteria was performed following the standard procedure. Biochemical properties for isolated bacteria were characterized using the kit from Hangzhou Microbiological Reagents Limited Company (Hangzhou, China) following the manufacturer's instructions.

2.5. Molecular identification for pathogen

PCR was performed to amplify the potential pseudorabies virus (PRV) and bacteria sequence using PRV conserved primers and bacterial 16S rRNA primers listed in Table 1. PCR products were sequenced by Sangon Biotech Company (Sangon Biotech, Shanghai).

Table 1
primers used for amplification of potential pseudorabies virus and bacteria.

Name	Sequence(5'→3')	Expected size
PRV-F	AGGAGACCATCCTGGTGTGTGCGAG	589bp
PRV-R	CGCGTCAGCACCAGCTGGGCCA	
16SrRNA-27F	AGAGTTTGATCMTGGCTCAG	1800bp
16SrRNA-1492R	TACGGYTACCTTGTTACGACTT	

2.6. Determination of pathogenicity

Mice in group I to IV were intraperitoneally inoculated with bacteria of 10^5, 10^6, 10^7 and 10^8 cfu/0.1 ml, respectively. Mice in group V were used as control group with each mouse was injected with 0.1 ml phosphate-buffered saline (PBS). After administration, mice were observed every 4–6 h. The minimal lethal dose (MLD) was determined according to the morbidity and mortality rate of mice in each group.

2.7. Tissue processing and H&E staining

Tissue samples for histopathological analysis were processed following standard procedure as previously reported [18]. Briefly, formalin-fixed tissues were dehydrated in a series of increasing concentrations of ethanol (70%, 80%, 95% and 100%) before they were incubated in Xylene (Thermo Fisher Scientific) two times with each time incubating for 1 h at room temperature, and then infiltrated with melted paraffin wax in an oven at 65 °C. Paraffin-embedded tissue blocks were sectioned at 5 μm using a microtome. The sections were loaded to polylysine-coated glass slides, dried overnight at 42 °C, and stored at room temperature for further use. Hematoxylin and Eosin (H&E) staining was performed following the standard procedures. Lesions were visualized and captured using a CCD camera mounted on a Nikon epifluorescence microscope (Nikon Instruments Co., Ltd, Shanghai).

2.8. TNF-α assay

The brain tissues were weighed and homogenized with PBS (w/v, 1:9) on ice before centrifugation at 12,000 rpm for 15 min at 4 °C. The supernatant was collected and used for detection of TNF-α expression using enzyme-linked immunosorbent assay (ELISA) kit per the manufacturer's protocol (BioLegend, Inc., San Diego, CA, USA).

2.9. Western blot assay

Brain samples were collected and homogenized. Total protein was extracted using T-PER tissue protein extraction reagent kit following the manufacturer's protocol. Equal amount of total proteins was loaded and separated in SDS-PAGE gel before transferred onto polyvinylidene difluoride (PVDF) membrane. The membranes were probed with primary antibodies after blocking in 5% nonfat milk, and then incubated with secondary antibody for 1 h at room temperature. The signals in blots were developed using a western blot detection program and captured using the ECL Plus Western Blotting Detection System (Amersham Life Science, UK). α-tubulin was used as an internal control.

2.10. Statistical analysis

All experiments were repeated at least three times. Data were expressed as the mean ± standard deviation (SD). Differences between the mean values of normally distributed data were assessed with the two-tailed Student's *t*-test p values of ≤ 0.05 were considered statistically significant.

3. Results

3.1. Epidemiological investigations and clinical manifestations

The patients (dogs) was reported to show listlessness, anorexia, and nervous disorder like seizure and epilepsy before the sudden death. Epidemiological data revealed the patients likely had the opportunity of contacting to pigs infected by pseudorabies virus on a nearby pig farm. The patients were brought to the Veterinary Hospital affiliated to the College of Veterinary Medicine at Jilin University within two hours after death. Initial examination found they were in a very good nutrition with smooth/shining furs, and the possibility for dogs to contact

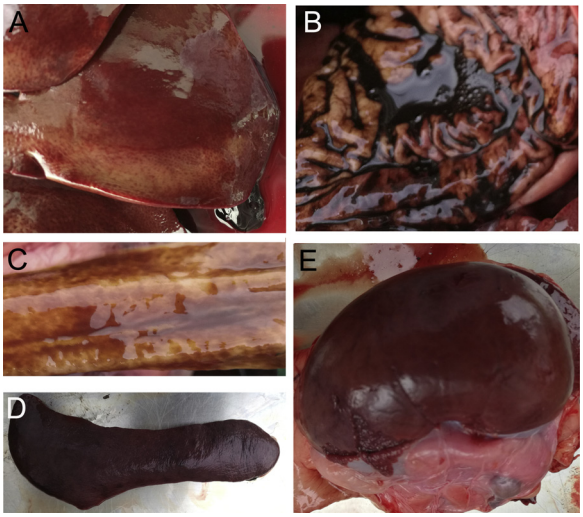

Fig. 1. Representative figure shows the main pathological lesions in dogs. Autopsy was performed to examine the gross lesions from the dead dog. Liver swollen with diffused hemorrhage (A). Gastric mucosa swollen and stomach filled with a large amount of gas and tar-like contents (B). Swollen mucosa in intestine filled with gas and coal tar-like contents (C). Infarction and hemorrhagic spots in spleen (D). Kidney swollen and fragile (E).

rodenticides were also excluded.

3.2. Gross lesions

To determine the potential causes, autopsies were performed for the patients. As shown in Fig. 1, gross lesions were observed including a swollen liver with diffused hemorrhage (Fig. 1A). Stomach was filled with a large amount of gas and coal tar-like contents, with gastric mucosa swollen (Fig. 1B). Small intestine was also filled with gas and coal tar-like stuffs with a thick intestinal mucosa (Fig. 1C). Infarction and hemorrhagic spots were observed in spleen (Fig.1D). Kidney was swollen and fragile (Fig. 1E). Edema and petechial hemorrhage were observed in the meninges of brain (data not shown).

3.3. Detection of the potential pathogens

To determine the potential pathogens, tissue samples of liver, lung, brain, spleen, pericardial fluid, and blood were collected under aseptic conditions. Smear slides were prepared and stained with Gram-staining. As shown in Table 2, it is surprising to note that a variety amount of small rod-shape bacteria were observed in almost all samples, especially in the brain sample. These results suggested the possibility of the bacteria involved in this disease, existence of bacteremia, and the capability of bacteria to penetrate the BBB.

Table 2
Bacterial counts on the smear tissue samples from infected dogs.

Sample	Relative bacterial counts
liver	+ +
lung	+
brain	+ + +
spleen	+ +
pericardial fluids	–
blood	+

- refers to negative; + stands for scattered bacteria; + + stands for a small number of bacteria; + + + refers to a large quantity of bacteria.

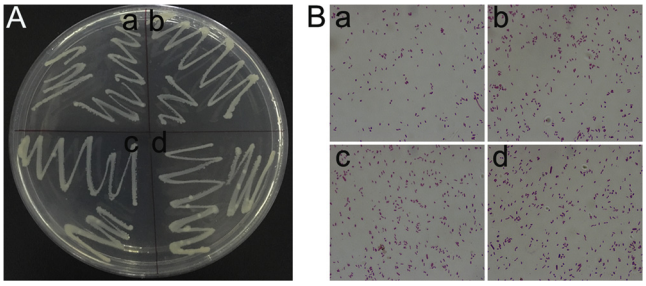

Fig. 2. Isolation and identification of potential bacterial pathogen. Large, thick, greyish white, smooth, moisture colonies grown in LB plates containing 2% FBS in tissue sample of liver (A-a), brain (A-b), spleen (A-c), and lung (A-d). Gram-negative, rod-shaped bacillus revealed in colonies isolated from liver (B-a), brain (B-b), spleen (B-c), and lung (B-d).

3.4. Bacteria isolation

To identify the bacteria, isolation was performed from the samples mentioned above. As shown in Fig. 2A, bacteria were isolated from samples of liver, brain, spleen, and lung collected aseptically using the LB agar plate containing 2% FBS. After streaking and incubating the plates at 37°C for 14 h, many large, thick, greyish white, smooth, moisture colonies were observed. Further staining the bacterial colonies with Gram staining showed the isolated bacterial colonies had the same morphology with the bacteria observed in tissue samples. They were pure small, straight, Gram-negative rod-shaped bacillus (Fig. 2B).

3.5. Biochemical properties

To characterize the isolate bacteria, biochemical properties were performed following manufacture's instruction. The isolates had the capacity of decomposing indole, methyl red, sorbitol, xylose, lysine, ornithine. However, they did not decompose citrate, VP, urea, phenylalanine, and hydrogen sulfide.

3.6. The isolated bacteria are E. coli

To determine the bacteria molecularly, the primers for bacterial 16S rRNA were used to amplify the genome sequence of the isolated bacteria. As expected, a fragment with a size of 1.8 kb was amplified

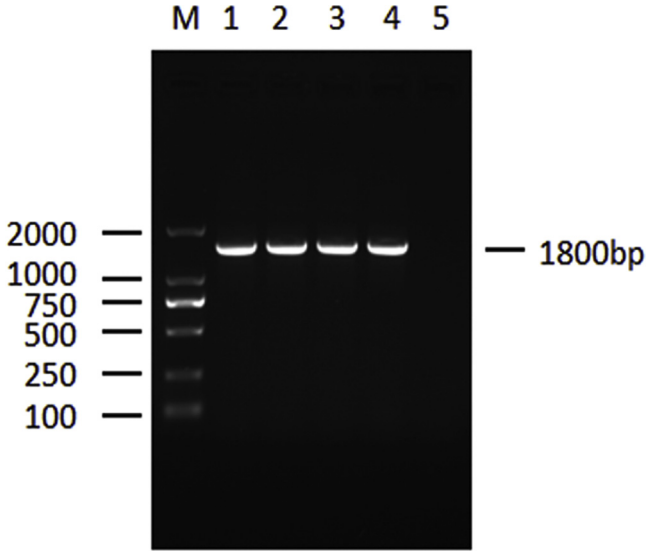

Fig. 3. Amplification of 16S rRNA gene from isolated pathogens. A fragment was amplified in liver (Lane 1), brain (Lane 2), spleen (Lane 3), lung (Lane 4), negative control (Lane 5). Lane M stands for a DNA ladder.

(Fig. 3). Sequencing the fragment showed that the fragment contained the sequence up to 99% sequence identity with *E. coli*, suggesting the isolated bacteria were *E. coli*. The isolated bacteria were named as CEC-GZL17.

Since initial epidemiological investigation indicated that the patients probably contacted the pigs with PRV infection, PRV-specific primers were used to amplify the potential viruses. No fragments were amplified from the mixed samples of liver, spleen, kidney, brain and lung using PCR, ruling out the possibility that PRV was involved in the disease (data not shown). No virus particles were observed after the above mixed samples were examined using EM, further excluding the involvement of viruses in the disease.

3.7. CEC-GZL17 was highly pathogenic

To determine the pathogenicity and minimal lethal dose for CEC-GZL17, a murine model system was employed. Mice were inoculated intraperitoneally using different colony forming units (cfu) of CEC-GZL17 bacteria diluted in PBS, with the control mice inoculated intraperitoneally with equal volume of PBS. After inoculation, mice infected with CEC-GZL17 bacteria showed restlessness in early hours, and had discharge in eyes and manifested conjunctivitis 10–12 h post infection. Some mice also showed dyspnea. The mice died in 12–14 h post infection after inoculation of 1.0×10^8 cfu and 1.0×10^7cfu/0.1 ml of log phase CEC-GZL17 bacteria, and became dead in 24–48 h after infection of 1.0×10^6 cfu/0.1 ml of CEC-GZL17 (Fig. 4). Similar to the mice in the control group, the mice inoculated with 1.0×10^5 cfu/0.1 ml of CEC-GZL17 were all survived. The minimal lethal dose of CEC-GZL17 was 1.0×10^6 cfu.

3.8. Recovery of CEC-GZL17 bacteria from the infected mice

To recover the bacteria, tissues from infected mice were collected and used for detection and isolation of the CEC-GZL17 bacteria. As shown in Fig. 5, a large number of gram-negative small-rod like bacilli were observed in the smear slides made from the organs and tissues, especially from the brain, indicating the bacteria were indeed responsible for the death of the infected mice. Detection of a large number of bacteria in the brain tissue suggests that CEC-GZL17 bacteria have the capability of crossing through the BBB. Further characterization of the recovered bacteria from the infected mice showed that they had the same characters to the bacteria isolated from dogs (data not shown).

3.9. Pathological lesions in mice

To further define if the mice infected with CEC-GZL17 bacteria shared the similar pathological characters, autopsy of the mice were performed following a standard protocol. As shown in Fig. 6, infected mice displayed an enlarged and fragile liver (Fig. 6A). Hemorrhagic spots were observed in spleen (Fig. 6B). Intestines were filled with gas (Fig. 6C). Edema was observed in the brain (Fig. 6D).

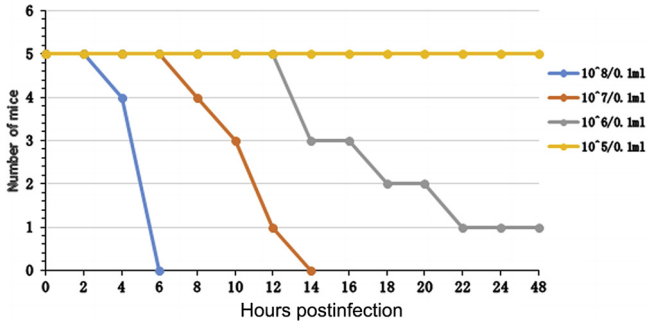

Fig. 4. Pathogenicity of CEC-GZL17 to mice. Mice were experimentally infected with different doses of isolated bacteria CEC-GZL17 strain. Morbidity and mortality were calculated based on the presence or absence of clinical signs, and death hours post infection, respectively. Axis X and Y present the number of mice survived and the hours post infection, respectively.

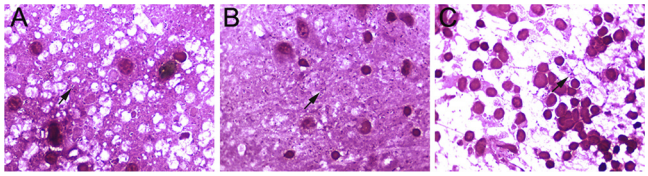

Fig. 5. Examination of the bacteria from mice infected by CEC-GZL17. Representative figure showing the Gram-negative bacteria observed in liver (A), brain (B) and spleen (C) in mice infected by CEC-GZL17.

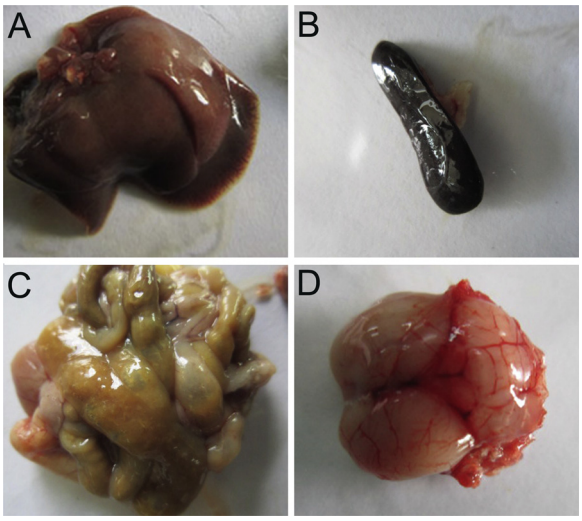

Fig. 6. Gross lesions in mice infected with CEC-GZL17. Representative figure showing the pathological lesions in infected mice, with an enlarged and fragile liver (A), spleen with hemorrhagic spot (B), intestinal gas (C), and cerebral edema (D).

Histopathological examinations revealed necrosis and congestion in liver (Fig. 7A-B) and spleen (Fig. 7D,E). A large number of inflammation cells were observed in lung with bronchi filled with the detached epithelial cells (Fig. 7G,H). Swelling and necrosis were also observed in kidney, especially for the epithelial cells in distal and proximal convoluted tubules (Fig. 7J,K). Intensive edema and necrosis with the heavily stained condensed nuclei were shown in nerve cells (Fig. 7M,N).

3.10. Increase of TNF-α and NF-κB P65 expression in mice infected by CEC-GZL17

To explore the mechanisms for CEC-GZL17 to cross through the blood-brain barrier, the TNF-α expression in brain tissue was initially assayed by ELISA. As shown in Fig. 8, TNF-α expression was significantly increased after CEC-GZL17 infection in comparison with the control group. Similarly, phosphorylation of NF-κB P65 was also significantly increased (Fig. 9). Those results indicate that NF-κB likely plays an important role in CEC-GZL17 bacteria-mediated inflammation and the dysfunction of the blood-brain barrier.

3.11. Decrease of ZO-1 and occludin expression in brain tissue of mice infected by CEC-GZL17

The blood-brain barrier consists of tight junctions around the capillaries and acts effectively to protect the brain from circulating pathogens. Loss of tight junction is directly correlated with the blood-

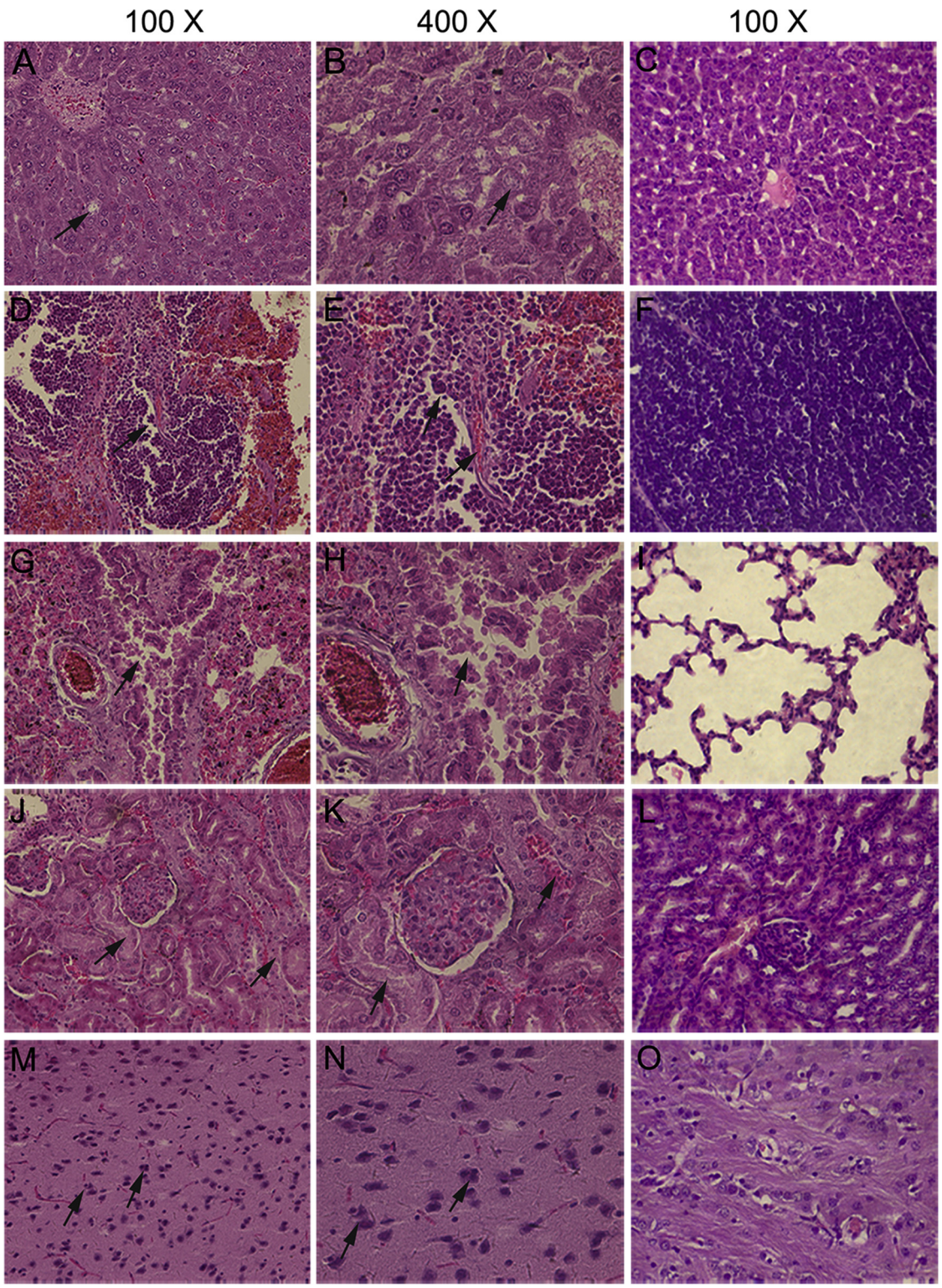

Fig. 7. Histopathological lesions in mice infected by CEC-GZL17. Representative figure showing the necrosis and congestion in liver (A, B) and spleen (D, E) compared with the normal tissues (C, F). A large number of inflammatory cells infiltrated in lung tissue and detached epithelial cells filled in bronchi (G, H). Necrosis and disruption of tissue structure in kidney (J, K). Intensive edema and necrosis in nerve cells with the heavily stained condensed nuclei (M, N). The normal control for lung, kidney and brain were shown in Fig I, L and O.

brain barrier dysfunction [19]. To further elucidate the mechanism underlying the disruption of the blood-brain barrier by CEC-GZL17 infection, the tight junction protein expressions were examined in brain tissue of the mice infected by CEC-GZL17. As illustrated in Fig. 9, the ZO-1and occludin expressions were significantly decreased in mice infected by CEC-GZL17 compared with the control group. These findings indicate that the CEC-GZL17 infection results in the degradation of TJ proteins, thus leading to the disruption of blood-brain barrier and the invasion of bacteria to brain tissue.

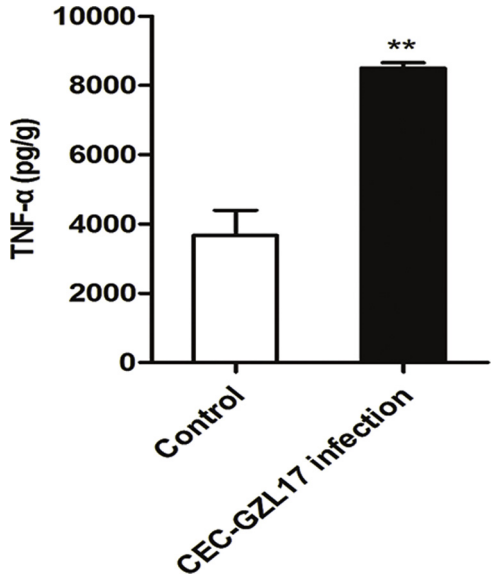

Fig. 8. Increase of TNF-α expression in brain tissue. TNF-α expression in brain tissue was measured by ELISA. Values are mean ± SD. $^{*}p < 0.05$ and $^{**}p < 0.01$ vs the control group.

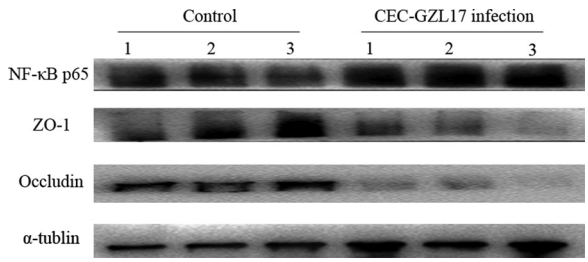

Fig. 9. Modulation of the expression of NF-κBp65, ZO-1 and occludin in brain tissue. Protein levels of NF-κB p65, ZO-1 and occludin in brain were analyzed by western blotting. α-tublin was used as a control (n = 3).

4. Discussion

In this study, we reported the isolation and characterization of the *E. coli* bacteria CEC-GZL17 from dogs characterized by septicemia and nervous system disorder, and demonstrated the isolated *E.coli* had the capability of causing septicemia and meningoencephalitis using a murine model system. We also demonstrated that CEC-GZL17 harbors the capability of disrupting the blood-brain barrier via down-regulating the expression of tight junction protein expression.

Infection of *E. coli* under certain circumstance poses a severe threat to public health and livestock industry. Although *E. coli* infection has been increasingly reported in a variety of animal species [20–22], it is less reported in dogs, especially on the clinical type characterized by septicemia and meningoencephalitis. Our results of PCR amplification and sequencing of 16 rRNA gene showed CEC-GZL17 shared 99% homology with that of *E. coli,* suggesting it is an *E.coli* bacteria. Experimental infection of mice by the isolated bacteria revealed the pathogenicity of CEC-GZL17. More interestingly, examination of the infected mice tissues revealed a large number of *E.coli* bacteria in the samples of liver, lung, spleen and pericardial fluid. It needs to mention that a huge number of *E.coli* bacteria were also observed in the brain tissue. These results clearly demonstrated the pathogenicity and the capability of CEC-GZL17 to penetrating the blood-brain barrier and causing the meningoencephalitis in infected mice, and the dogs as well. Although early studies demonstrated that *E. coli* was able to invade different tissues in a variety of animal species [23,24], the case reported in this study for *E.coli* bacteria to cause canine septicemia and meningoencephalitis was seldomly reported. Our report will broaden the understanding of *E.coli* as an important pathogen associated with septicemia and meningoencephalitis.

The blood-brain barrier is a highly selective semipermeable membrane barrier that separates the circulating blood from the brain and extracellular fluid in the central nervous system (CNS) and protects the brain from potential bacteria in the blood [25,26]. To determine the potential mechanisms of meningoencephalitis underlying CEC-GZL17 infection, the mice model system was employed. Our findings showed that CEC-GZL17 infection significantly decreased the tight junction protein ZO-1 and occludin expression. As ZO-1 and occludin tight junction molecules are crucial for the structural and functional integrity of the blood-brain barrier in brain tissue, the down-regulation of these proteins indicates that CEC-GZL17 infection likely enhances the permeability of blood-brain barrier and increases CEC-GZL17 across the blood-brain barrier, thus resulting in meningoencephalitis. In addition, since TNF-α is the earliest and most important inflammatory mediator that activates neutrophils and lymphocytes and increases the permeability of vascular endothelial cells in the process of inflammation, the finding that CEC-GZL17 infection significantly increases TNF-α expression in brain tissue further indicates that CEC-GZL17-associated meningoencephalitis is likely due to the increase of TNF-α expression in brain tissue, this is consistent with the results as reported by other studies [27–29]. Furthermore, NF-κB is a protein complex involved in cellular response to many extracellular stimuli including to infection. Once activated, NF-κB induces the production of pro-inflammatory cytokines, such as TNF-α [30]. We detected the increased expression of phosphorylated NF-κB p65, indicating CEC-GZL17-induced meningoencephalitis is probably related to NF-κB signal. Although we did not know the exact resource where the dogs got infected with the pathogenic CEC-GZL17, the evidence we provided demonstrated that CEC-GZL17 have the capability of causing septicemia and meningoencephalitis, and penetrating the blood-brain barrier.

In summary, we demonstrated that *E. coli* strain CEC-GZL17 is the causative agents associated with the rare canine septicemia and meningoencephalitis, where attention should be paid by veterinary practitioners. Our results demonstrated that CEC-GZL17 likely employs the mechanism by disruption of the blood-brain barrier through down-regulating the expression of the tight junction protein in the brain tissue, thus leading to the meningoencephalitis.

Conflict of interest

The authors declare no conflict of interest.

Acknowledgements

This study is supported by the National Key Research & Development Program 2017YFD0500104 and 2016YFD0500904 from the Ministry of Science and Technology of People's Republic of China. We thank Li Yang at the Jilin University for her help in examining the potential viral pathogens using EM.

References

[1] O. Tenaillon, D. Skurnik, B. Picard, E. Denamur, The population genetics of commensal Escherichia coli, Nat. Rev. Microbiol. 8 (2010) 207–217.
[2] M. Accogli, D. Fortini, M. Giufre, C. Graziani, M. Dolejska, A. Carattoli, et al., IncI1 plasmids associated with the spread of CMY-2, CTX-M-1 and SHV-12 in Escherichia coli of animal and human origin, Clin. Microbiol. Inf. 19 (2013) E238–E240.
[3] L. Ouchenir, C. Renaud, S. Khan, A. Bitnun, A.A. Boisvert, J. McDonald, et al., The epidemiology, management, and outcomes of bacterial meningitis in infants, Pediatrics (2017) 140.
[4] M. Riveros, W. Garcia, C. Garcia, D. Durand, E. Mercado, J. Ruiz, et al., Molecular and phenotypic characterization of Diarrheagenic escherichia coli strains isolated from bacteremic children, Am. J. Trop. Med. Hyg. 97 (2017) 1329–1336.
[5] J.A. Veltman, C.C. Bristow, J.D. Klausner, Meningitis in HIV-positive patients in sub-Saharan Africa: a review, J. Int. AIDS Soc. 17 (2014) 19184.
[6] Z. Pan, J. Ma, W. Dong, W. Song, K. Wang, C. Lu, et al., Novel variant serotype of

streptococcus suis isolated from piglets with meningitis, Appl. Environ. Microbiol. 81 (2015) 976–985.
[7] H. Ghunaim, M.A. Abdelhamid, S. Kariyawasam, Advances in vaccination against avian pathogenic Escherichia coli respiratory disease: potentials and limitations, Vet. Microbiol. 172 (2014) 13–22.
[8] D.V. Mukherjee, J.H. Tonry, K.S. Kim, N. Ramarao, T.G. Popova, C. Bailey, et al., Bacillus anthracis protease InhA increases blood-brain barrier permeability and contributes to cerebral hemorrhages, PLoS One 6 (2011) e17921.
[9] L.Y. Chen, Y.X. Xue, J. Zheng, X.B. Liu, J. Liu, J.J. Chen, et al., MiR-429 Regulated by Endothelial Monocyte Activating Polypeptide-II (EMAP-II) Influences Blood-Tumor Barrier Permeability by Inhibiting the Expressions of ZO-1, Occludin and Claudin-5, Front. Mol. Neurosci. (2018) 11.
[10] Y. Cheng, S. Desse, A. Martinez, R.J. Worthen, R.S. Jope, E. Beurel, TNFalpha disrupts blood brain barrier integrity to maintain prolonged depressive-like behavior in mice. Brain, behavior, Immunity 69 (2018) 556–567.
[11] G. Ramesh, A.G. MacLean, M.T. Philipp, Cytokines and chemokines at the crossroads of neuroinflammation, neurodegeneration, and neuropathic pain, Mediators Inflamm. (2013).
[12] M. Aslam, N. Ahmad, R. Srivastava, B. Hemmer, TNF-alpha induced NF kappa B signaling and p65 (RelA) overexpression repress Cldn5 promoter in mouse brain endothelial cells, Cytokine 57 (2012) 269–275.
[13] B. Zhuan, Y. Yu, Z. Yang, X. Zhao, P. Li, Mechanisms of oxidative stress effects of the NADPH oxidase-ROS-NF-kappaB transduction pathway and VPO1 on patients with chronic obstructive pulmonary disease combined with pulmonary hypertension, Eur. Rev. Med. Pharmacol. Sci. 21 (2017) 3459–3464.
[14] Z. Zhang, P. Shen, X. Lu, Y. Li, J. Liu, B. Liu, et al., In vivo and in vitro study on the efficacy of Terpinen-4-ol in dextran sulfate sodium-induced mice experimental colitis, Front. Immunol. 8 (2017) 558.
[15] H. Ji, X. Zhang, Y. Du, H. Liu, S. Li, L. Li, Polydatin modulates inflammation by decreasing NF-kappaB activation and oxidative stress by increasing Gli1, Ptch1, SOD1 expression and ameliorates blood-brain barrier permeability for its neuroprotective effect in pMCAO rat brain, Brain Res. Bull. 87 (2012) 50–59.
[16] X. Zhang, X. Zhang, C. Wang, Y. Li, L. Dong, L. Cui, et al., Neuroprotection of early and short-time applying berberine in the acute phase of cerebral ischemia: up-regulated pAkt, pGSK and pCREB, down-regulated NF-kappaB expression, ameliorated BBB permeability, Brain Res. 1459 (2012) 61–70.
[17] T.Q. An, J.M. Peng, Z.J. Tian, H.Y. Zhao, N. Li, Y.M. Liu, et al., Pseudorabies virus variant in Bartha-K61-Vaccinated pigs, China, Emerg Infect Dis. 2013 (19) (2012) 1749–1755.
[18] X.P. Wang, X.L. Deng, X.C. Zhang, Identification of a novel splicing form of amelogenin gene in a reptile, Ctenosaura similis, PLoS One 7 (2012).
[19] B.T. Hawkins, T.P. Davis, The blood-brain barrier/neurovascular unit in health and disease, Pharmacol. Rev. 57 (2005) 173–185.
[20] S. Krishnan, A.C. Chang, J. Hodges, P.O. Couraud, I.A. Romero, B. Weksler, et al., Serotype O18 avian pathogenic and neonatal meningitis Escherichia coli strains employ similar pathogenic strategies for the onset of meningitis, Virulence 6 (2015) 777–786.
[21] X.B. Wang, C.G. Cao, H.X. Huan, L.L. Zhang, X.H. Mu, Q.Q. Gao, et al., Isolation, identification, and pathogenicity of O142 avian pathogenic Escherichia coli causing black proventriculus and septicemia in broiler breeders, Infect. Genet. Evol. 32 (2015) 23–29.
[22] M.T. Boubezari, T. Idoui, R. Hammami, B. Fernandez, A. Gomaa, I. Fliss, Bacteriocinogenic properties of Escherichia coli P2C isolated from pig gastrointestinal tract: purification and characterization of microcin V, Arch. Microbiol. (2018).
[23] Z.R. Stromberg, J.R. Johnson, J.M. Fairbrother, J. Kilbourne, A. Van Goor, R. Curtiss, et al., Evaluation of Escherichia coli isolates from healthy chickens to determine their potential risk to poultry and human health, PLoS One (2017) 12.
[24] W.C. Shen, X. Wang, W.T. Qin, X.F. Qiu, B.W. Sun, Exogenous carbon monoxide suppresses Escherichia coli vitality and improves survival in an Escherichia coli-induced murine sepsis model, Acta Pharmacol. Sin. 35 (2014) 1566–1576.
[25] H.C. Helms, N.J. Abbott, M. Burek, R. Cecchelli, P.O. Couraud, M.A. Deli, et al., In vitro models of the blood-brain barrier: an overview of commonly used brain endothelial cell culture models and guidelines for their use, J. Cereb. Blood Flow Metab. 36 (2016) 862–890.
[26] X. Chen, S.W. Threlkeld, E.E. Cummings, I. Juan, O. Makeyev, W.G. Besio, et al., Ischemia-reperfusion impairs blood-brain barrier function and alters tight junction protein expression in the ovine fetus, Neuroscience 226 (2012) 89–100.
[27] M.K. Connolly, A.S. Bedrosian, J.M.S. Clair, A.P. Mitchell, J. Ibrahim, A. Stroud, et al., In liver fibrosis, dendritic cells govern hepatic inflammation in mice via TNF-alpha, J. Clin. Invest. 119 (2009) 3213–3225.
[28] B.H. Maskrey, I.L. Megson, P.D. Whitfield, A.G. Rossi, Mechanisms of resolution of inflammation a focus on cardiovascular disease, Arterioscl Throm Vas. 31 (2011) 1001–1006.
[29] G.A. Duque, A. Descoteaux, Macrophage cytokines: involvement in immunity and infectious diseases, Front. Immunol. 5 (2014) 1–12.
[30] H.L. Pahl, Activators and target genes of Rel/NF-kappa B transcription factors, Oncogene 18 (1999) 6853–6866.